

Utilization of SPOT 5 data for mapping gold mineralized diorite–tonalite intrusion, Bulghah gold mine area, Saudi Arabia

Hesham Harbi · Ahmed Madani

Received: 17 September 2012 / Accepted: 19 July 2013 / Published online: 7 August 2013
© Saudi Society for Geosciences 2013

Abstract The present study utilizes the processed SPOT 5 data to discriminate and to generate 1:10,000 geologic image map to delineate the mineralized diorite–tonalite intrusion around Bulghah gold mine area, Saudi Arabia. The rock units exposed in the area include gossan, marble, Hulayfah volcanics, diorite–tonalite, gneissose granite, and alkali granite. Gold mineralization at Bulghah mine is hosted mainly by Syn- to Late-tectonic diorite–tonalite intrusion aligned along N–S direction and is associated mainly with cataclastic zones and quartz veins. Gossans and jasperoidal gossans (Hulayfah group), recorded at the western side of Bulghah mine area as discontinuous small lenses, can be easily discriminated on 4/2 and 4/3 band ratio SPOT images by their white and black image signatures, respectively. Granitoids (gneissose granite and alkali granite) are easily discriminated in 3/2 ratio image, in which gneissose granite has gray image signature, whereas alkali granite has dark gray image signature. On the SPOT false color composite band ratios image (3/2 R, 4/2 G, and 4/3 B), gossan, marble, Hulayfah volcanics, diorite–tonalite, gneissose granite, and alkali granite have sky blue, blood red, bluish light brown, orange, brick red, and deep blue colors, respectively. Fusion of the false color composite SPOT ratios image (3/2 R, 4/2 G, and 4/3 B) with the high spatial resolution SPOT pan image is performed using IHS transformation method. The fused image is used to delineate the mineralized diorite–tonalite intrusion and to produce 1:10,000 geologic image map for Bulghah gold mine area. The present study reveals the usefulness of the processed

SPOT 5 data for adding new extensions at the southern and northern boundaries of diorite–tonalite intrusion.

Keywords SPOT5 · Diorite–tonalite intrusion · Bulghah gold mine · Fusion technique

Introduction

The Late Proterozoic Arabian Shield was divided by several authors into five distinct terranes separated by four ophiolite-bearing suture zones. Three of these terranes represent ensimatic island arcs and are exposed in the western part of the shield (Asir, Hijaz, and Midyan), whereas the other two terranes (Afif and Ar Rayn) represent the continental affinity and exposed further to the east (Al Shanti and Mitchell 1976; Bakor et al. 1976; Greenwood et al. 1976; Frisch and Al Shanti 1977; Gass 1977, 1981; Schmidt et al. 1979; Camp 1984). Bulghah gold mine is situated at the western part of the Afif terrane to the east of the Nabitah suture zone, where Syn- to Late-tectonic diorite–granite plutons and their subvolcanic equivalents intrude Hulayfah, Siham, Murdama, and Bani Ghayy groups (Fig. 1; Sabir 1989; Leistel et al. 1999; Al Jahdali 2004; Harbi 2004). Gold mineralization at Bulghah area is represented by Bulghah gold mine and Bulghah North deposit. Bulghah mine started gold production on 2002. Extensive exploration activities by Maaden Company in 2005 led to the discovery of the Bulghah North and Humaymah deposits which are currently under exploration and evaluation. Mineralization is hosted primarily by Syn- to Late-tectonic diorite–tonalite intrusive body nearly striking in N–S direction and associated mainly with cataclastic zones, microfractures, and quartz veins. Mineralization in the Bulghah gold mine was the result of structurally focused hydrothermal fluid flow that occurred during regionally extensive crustal extensional deformation and associated with cataclastic fault development (Barnicoat et al. 1998). These

H. Harbi
Department of Mineral Resources and Rocks, Faculty of Earth Sciences, King Abdulaziz University, P.O. Box 80206, Jeddah 21589, Saudi Arabia

A. Madani (✉)
Water Research Center, King Abdulaziz University, P.O. BOX 80200, Jeddah 21589, Saudi Arabia
e-mail: aamadani18@hotmail.com

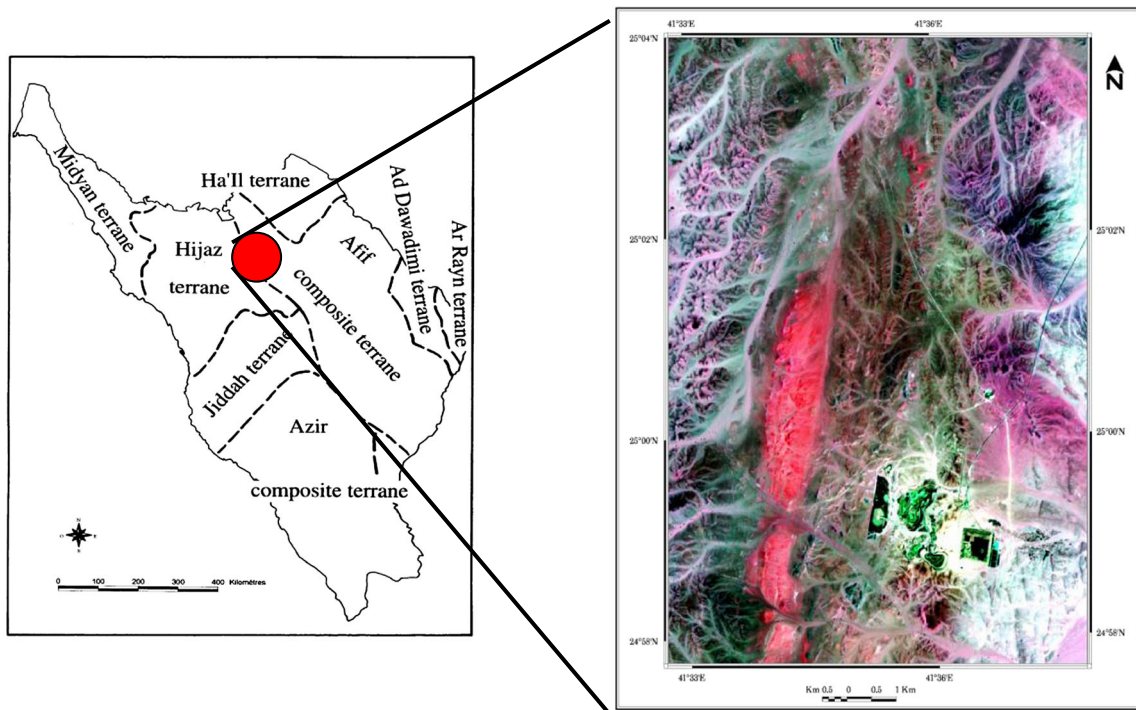
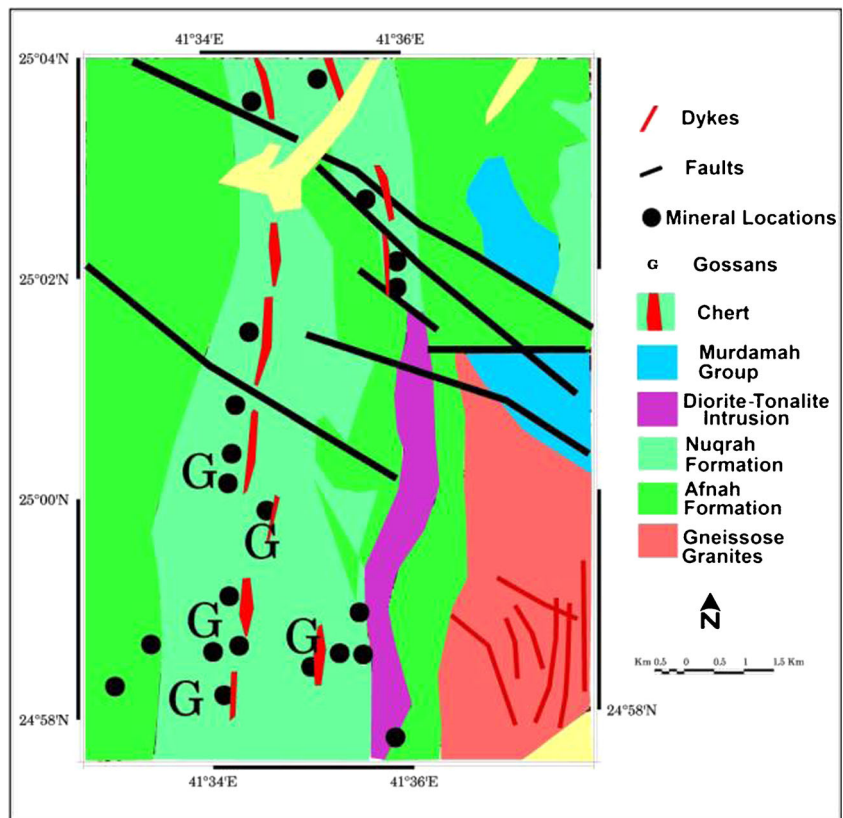


Fig. 1 Major terranes in the Arabian Shield and SPOT 5 false color composite image showing the location of the Bulghah gold mine area

deposits which have been classified as mesothermal vein-type gold mineralization (Agar 1992; Albino et al. 1995) formed in

association with intraplate settings and hosted in major secondary Najd fault system structures mostly in granitic

Fig. 2 Geological map of the study area extracted from the 1:250,000 geological maps of the Nuqrah and Al Hissu quadrangles compiled by Delfour (1977 and 1981), respectively



intrusions (Agar 1992). These deposits are characterized by low sulfide content typically represented by arsenopyrite, pyrite, and/or pyrrhotite (Harbi 2004). Gold occurs mainly as free microscopic gold along fractures or associated with sulfide grains in veins or in fractured alteration zones.

With the exception of the company reports, no detailed mapping is carried out on these gold deposits using satellite data. Comparison between Landsat data (high spectral resolution with

low spatial resolution) and SPOT 5 data (low spectral resolution with high spatial resolution) revealed the usefulness of the high-resolution SPOT 5 data for mining purposes in this study. The optimum scale obtained using Landsat ETM+ data is 1:100,000, and this scale is not suitable for mining stage and excluded from this study. The present paper utilizes the processed SPOT 5 data to generate 1:10,000 image map that delineate the new extensions of diorite–tonalite intrusion which host gold mineralization



Fig. 3 **a** Fine laminated tuffs, Nuqrah Formation. **b** Hematitic gossans (G) at the upper part of Nuqrah Formation. **c** Discontinuous marble ridges (MR) looking E. **d** Quartz veinlet (QZ) about 2 cm width within highly fractured cataclastic zone about 50 cm thick. **e** Brownish hematitic-clay

material along the N–S fault plane, Bulghah gold mine. Note the presence of two sets of fracture system NE and NW, looking N. **f** Andesitic dyke (AD) traversing diorite–tonalite intrusion (T), open-pit site–Bulghah North. Looking NW

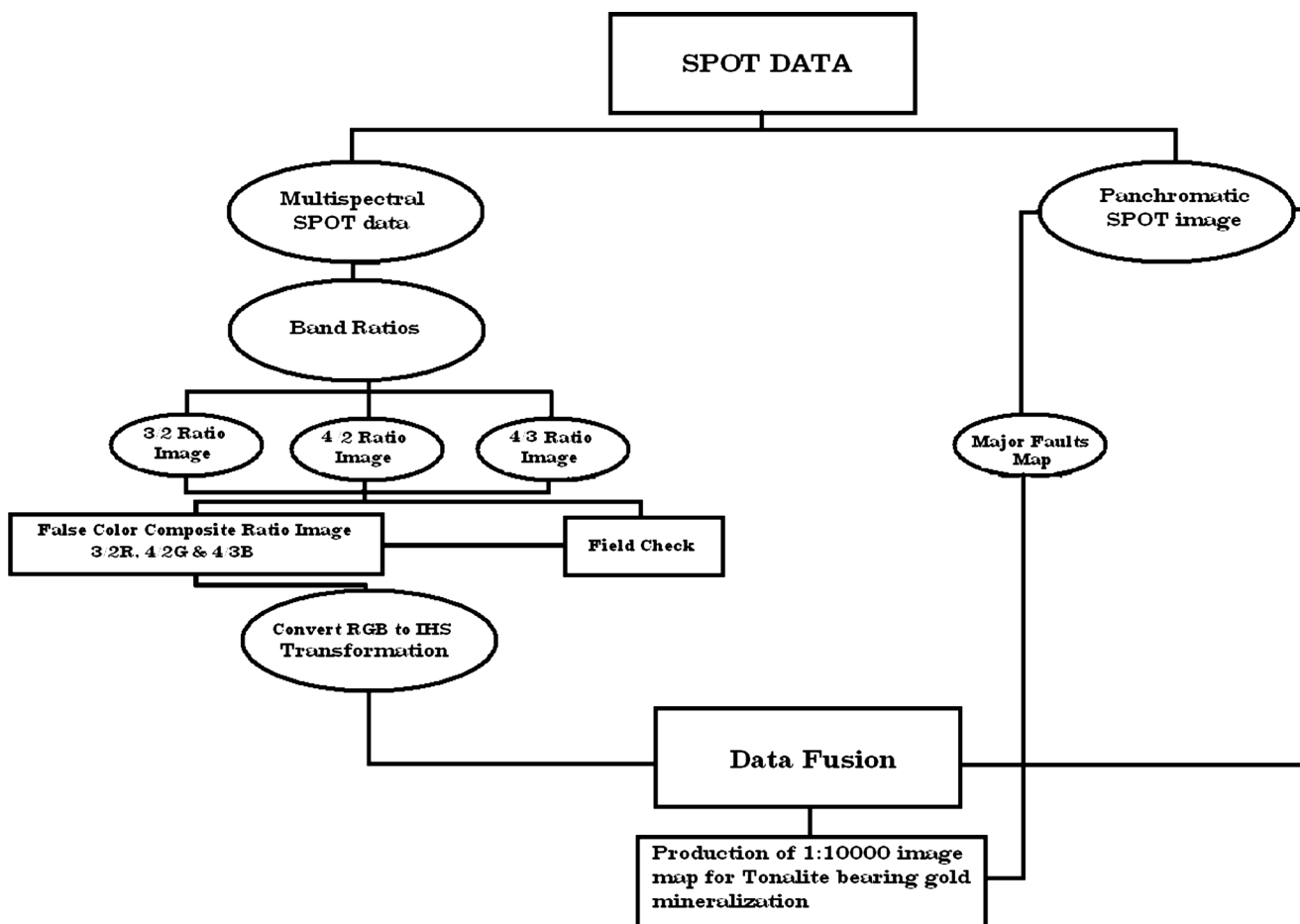


Fig. 4 Data processing flow chart demonstrates the main image processing techniques

exposed at Bulghah gold mine area. Two field trips were conducted for verification of the remote sensing analyses, collection of rock samples, and GPS readings.

Regional geology

A mosaic subset from Nuqrah and Al Hissu quadrangles (sheets 25E, GM-28, and 24E, GM-58) that covers the study area is shown in Fig. 2. A pronounced N–S extension of the mineralized diorite–tonalite intrusions is clearly observed in the middle of the mosaic.

Hulayfah group represents the oldest rock unit exposed at the study area and consists of older Afna Formation and younger Nuqrah Formation. Andesitic volcanic rocks and volcanoclastic derivatives commonly occur in the western and eastern part of the area and may represent rocks of Afna Formation. Nuqrah Formation is mostly represented by acidic volcanoclastic rocks including agglomerate, fine laminated tuffs (Fig. 3a), and intercalations of jasper and or cherty tuffs. Discontinuous small lenses of gossans and jasperoidal

gossans (Fig. 3b) are mostly exposed at the western part of the study area. Discontinuous marble bands forming nearly N–S to NNW trending ridges were exposed in the central part of the study area to the east of the diorite–tonalite intrusions (Fig. 3c). These marble ridges are exposed as small hills or moderately elevated bodies extending along the strike for tens

Table 1 SPOT 5 characteristics

| | |
|---------------------|--|
| Launch date | May 3, 2002 |
| Launch vehicle | Ariane 4 |
| Orbital altitude | 822 Km |
| Orbital inclination | 98.7°, sun-synchronous |
| Revisit time | 2–3 days, depending on latitude |
| Swath width | 60×60 Km to 80 Km at nadir |
| Resolution | Pan: 2.5 m from 2×5 m scenes Used data: Pan: 5 m (nadir), MS: 10 m (nadir) |
| Image bands | Pan: 480–710 nm, Green: 500–590 nm, Red: 610–680 nm Near IR: 780–890 μm, Shortwave IR: 1,580–1,750 μm |

of meters. They commonly occur within the middle part of the Nuqrah Formation in many parts of the Arabian Shield. The Hulayfah volcanics are unconformably overlain by Murdama Group rocks which are exposed at the eastern part of the study area and are represented by sandstone, conglomerate, rhyolite, andesite, and marble. Two main varieties of intrusive rocks belonging to Idah (620–615 Ma) and Abanat (585–570 Ma) suites intruded the previously described rock units. Previous studies (e.g., Eberte and Sahl 1999) considered the diorite–tonalite intrusion at Bulghah area to be similar to the diorite–tonalite intrusions hosting gold mineralization at Sukhaybrate area and assigned to Idah suite. Recent U–Pb Zircon SHRIMP dating (Harbi and McNaughton 2011) for two samples from the diorite–tonalite intrusion at Bulghah North and Bulghah mine area yield ages of 678 ± 16 and 667 ± 6 Ma, respectively. This indicates that the diorite–tonalite intrusions at Bulghah area are older than rocks of the Idah suite. These intrusive rocks which host gold mineralization at Bulghah area occupy the central part of the study area and occur as elongated body in NNE to N–S trend, 1 km width with 5 km length (see Fig. 2). Gold mineralization is mainly associated with cataclastic zones, microfractures, and quartz (\pm carbonate) veinlets (Fig. 3d). Several NW-trending andesite dykes with different widths (5 to 12 m) were recorded in the Bulghah north site. Aplitic veinlets with different widths are also observed having the same trend crosscut with the volcanics and the mineralized intrusive rocks. The second variety of the intrusive rocks is observed in the northern part of the study area and is represented by alkali granite.

Conjugate fault systems strike NE–SW and NW–SE directions, nearly vertical and about 20 cm in width, are observed in the Bulghah gold mine, which dissected the diorite–tonalite intrusion. They are characterized by the presence of brownish hematitic–clay material along the fault plane (Fig. 3e). Hybrid joint systems (extensional and shear) were recorded in the mine area. Three main kinds of dykes are easily recorded on SPOT 5 data, cutting the granitoid intrusions in the study area. The first kind is porphyritic andesite, about 10 m thick, has NW direction, and is recorded at the Bulghah north open-pit site cutting diorite–tonalite intrusion (Fig. 3f). The second type of dykes

has N–S direction and is represented by acidic dykes cutting pink alkali granite at the northeastern part of the study area. Pink acidic dykes that have NW direction were observed cutting gneissose granite to the east of Bulghah mine.

Methodology

The methodology adopted in this research includes digital processing of SPOT 5 and field measurements. Figure 4 shows the data processing flow chart, demonstrating the main image processing techniques performed throughout this study. Band ratio technique is performed on the subset of multispectral SPOT imagery which covers the study area. Visual inspection for the resultant ratio images revealed that 3/2, 4/2, and 4/3 band ratio images are the most informative ratios for lithologic discrimination and mapping. False color composite ratio image (3/2 R, 4/2 G, and 4/3 B) is generated and used in the field check. Data fusion between the above generated false color composite ratio image and the high spatial resolution panchromatic SPOT imagery is performed using the intensity–hue–saturation (IHS) transformation method. The fused image is verified and then used to delineate the new northern and southern extensions of diorite–tonalite bearing gold mineralization and to generate 1:10,000 image map for the study area. A subset of the panchromatic SPOT imagery that covers the study area is used to delineate the major structural elements affecting the study area.

Discrimination of diorite–tonalite intrusion using SPOT 5 band ratio images

SPOT 5 satellite was launched in May 2002 and is considered as the first high spatial resolution satellite with vast coverage area (2.5 m, 60×60 km). Table 1 shows the spectral and spatial characteristics of SPOT 5 data. Subsets from spectral and panchromatic SPOT 5 images for the study area were obtained using PCI software. Processing of high spatial resolution panchromatic SPOT imagery improves the identification and delineation of the main structural elements that may control mineralization in Bulghah gold mine area. Also, the moderate

Table 2 Image signatures and colors of the different rock units exposed at Bulghah gold mine area

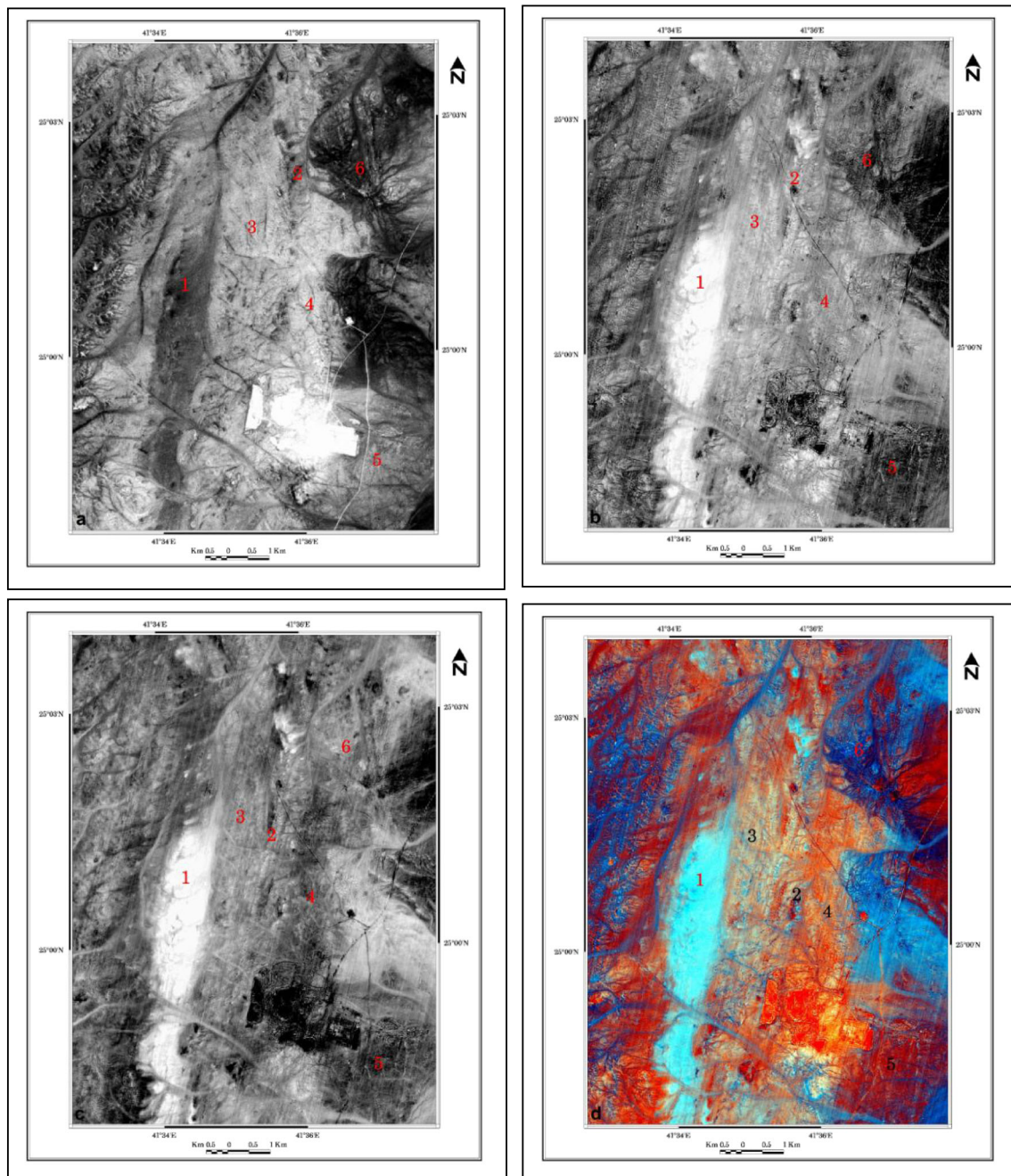
| | Gossan (1) | Marble (2) | Hulayfah volcanics (3) | Diorite/tonalite (4) | Gneissose granite (5) | Alkali granite (6) |
|------------------------------|------------|-----------------|------------------------|----------------------|-----------------------|--------------------|
| 3/2 ratio image | Dark gray | Very light gray | Gray | Light gray | Gray | Dark gray |
| 4/2 ratio image | White | Black | Light gray | Gray | Dark gray | Dark gray |
| 4/3 ratio image | White | Black | Gray | Dark gray | Dark gray | Gray |
| FCC 3/2 R, 4/2 G, and 4/3 B. | Sky blue | Blood red | Light brown | Orange | Brick Red | Deep blue |

spectral range (0.480 to 1,750 μm) helps in the discrimination of different lithologies at a great extent.

Band ratio, which is the main image processing technique used throughout this study, can be prepared simply by dividing the digital number (DN) values of each pixel in one band by the DN values of another band (Drury 1993). This process utilized the four multispectral spectral SPOT 5 bands under Geomatica v.9.1 environment. Visual inspection of the generated band ratio images revealed that the most informative ratios for lithologic

discrimination are 3/2, 4/2, and 4/3. Table 2 summarizes the image signatures for gossan, marble, Hulayfah volcanics, diorite–tonalite, gneissose granite, and alkali granite (numbers from 1 to 6 in the ratio images, respectively) as well as their colors on the SPOT false color composite ratio image 3/2 R, 4/2 G, and 4/3 B.

Figure 5a–c show the 3/2, 4/2, and 4/3 band ratio images. Gossan (1) and marble (2) are easily discriminated on 4/2 and 4/3 band ratio images by their white and black image



Figs. 5 a b, c, and d show the 3/2, 4/2, and 4/3 in gray color and FCC 3/2, 4/2, and 4/3 in RGB, respectively. 1 gossan, 2 marble, 3 volcanics, 4 diorite–tonalite, 5 gneissose granite, and 6 alkali granite

signatures, respectively. Granitoid rocks (gneissose granite (5) and alkali granite (6)) exhibit dark gray image signature on 4/2 and 4/3 images, whereas they are easily discriminated in 3/2 ratio image, in which gneissose granite has gray image signature; whereas alkali granite has dark gray image signature. Figure 5d shows the SPOT false color composite band ratios image 3/2, 4/2, and 4/3 in RGB in which gossan, marble, volcanics, tonalite, gneissose granite, and alkali granite exhibit sky blue, blood red, bluish light brown, orange, brick red, and deep blue colors, respectively.

Fusion technique and mapping of diorite–tonalite intrusion

Image fusion is the process of combining information from two or more images into a single composite image that is more informative and is more suitable for visual interpretation (Pohl and Van Genderen 1998; Wald 2002). The fused images can

provide information that sometimes cannot be observed in the individual input images. Image fusion algorithms (Fig. 6a) can be categorized into low-, mid-, and high-levels which may be referred to pixel, feature, and symbolic levels, respectively. Several works were done on pixel-level image fusion, whereas little works were done on feature and symbolic levels. Multi-resolution analysis is a popular method in pixel-level fusion. The most popular fusion algorithms are Brovey transformation, hue–saturation–value, IHS, principal component analysis, and wavelet transform (Carper et al. 1990; Chavez et al. 1991; Garguet-Duport et al. 1996; Li et al. 2002). In this study, fusion of the false color composite SPOT ratios image (3/2 R, 4/2 G, and 4/3 B) with the high spatial resolution SPOT pan image was performed using IHS transformation method. Figure 6b shows the main IHS fusion technique steps according to Ehlers (1991) method. This includes three main steps as follows: (1) transformation of the three multispectral

Fig. 6 a Image fusion at the pixel, object, and decision levels (after Pohl and Van Genderen 1998). b IHS fusion technique steps for the SPOT 5 data, modified after Ehlers 1991

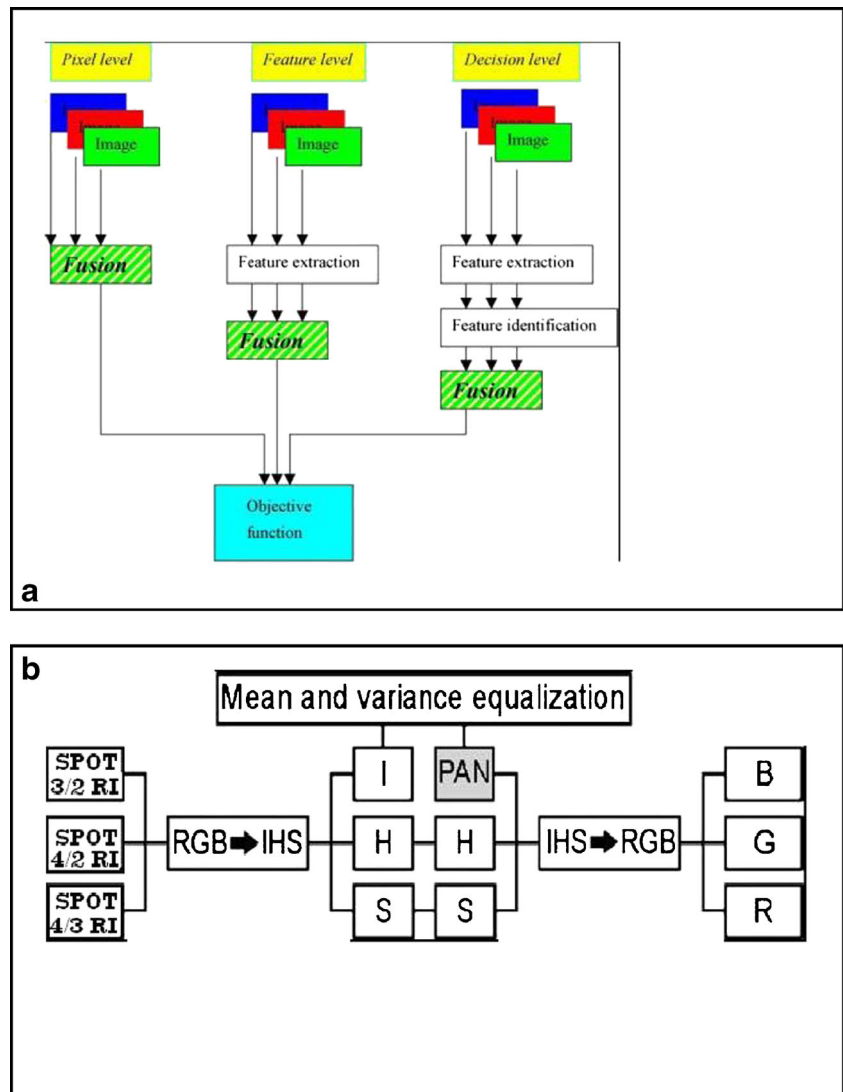


Fig. 7 Fused image for Bulghah gold mine area shows the northern extension of diorite-tonalite intrusion

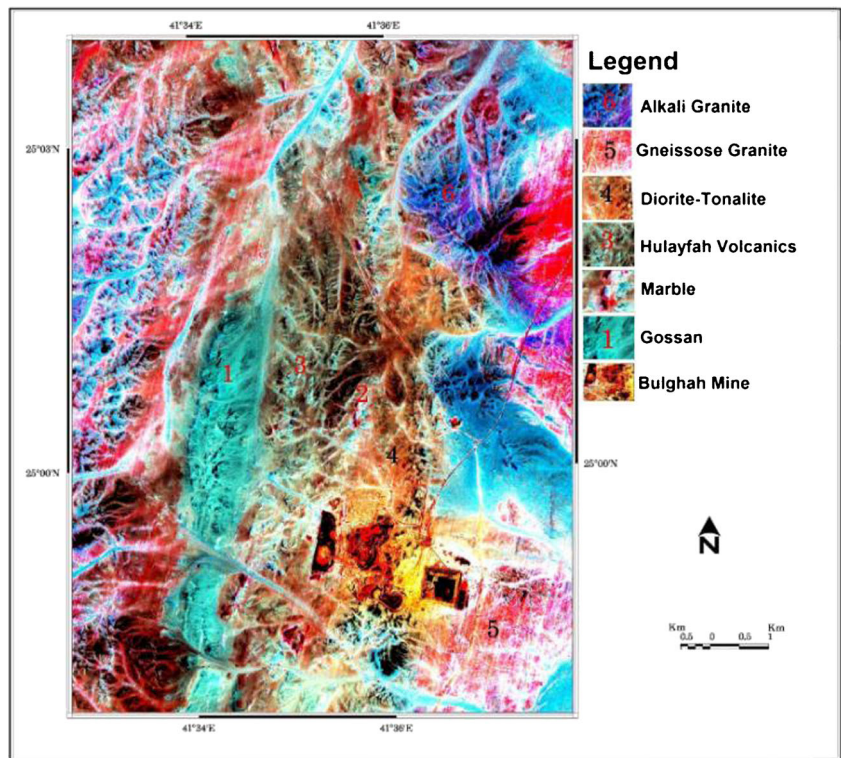
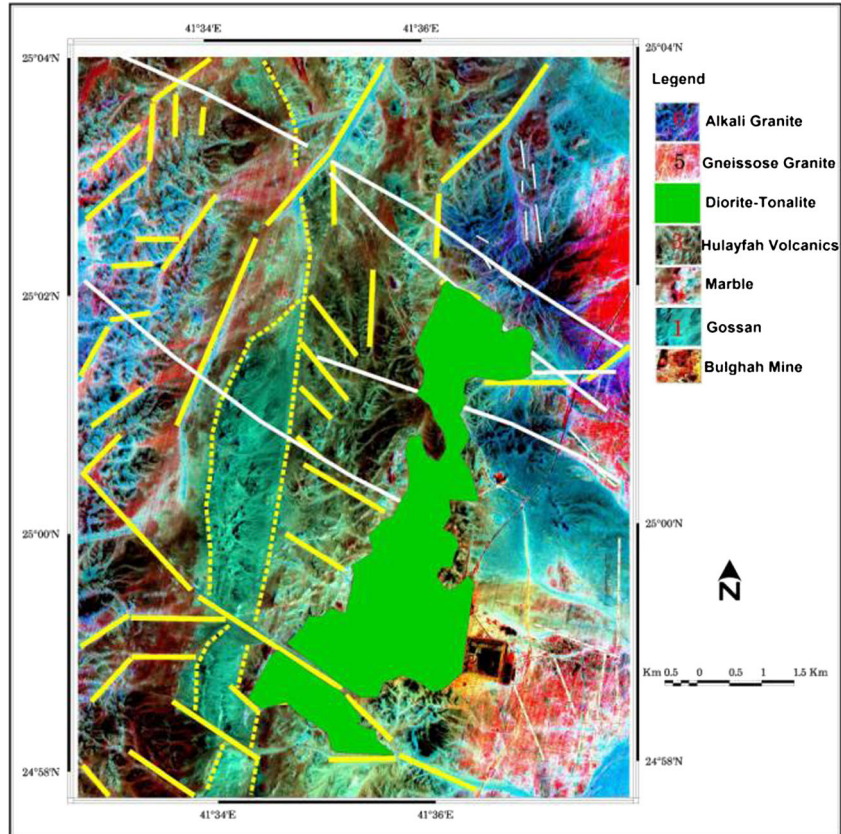


Fig. 8 Geological image map for the Bulghah gold mine area (1:10,000) shows the northern and southern extension of diorite-tonalite intrusion with the distribution of main fault systems



bands (SPOT ratio images 3/2, 4/2, and 4/3) from RGB to IHS color space, (2) substitution of intensity value (I) by the panchromatic SPOT band, and (3) back transformation from IHS to RGB. The resultant fused image is shown in Fig. 7 and is used to delineate diorite–tonalite intrusions bearing gold mineralization and to produce 1:10,000 geologic image map for Bulghah gold mine area (Fig. 8).

Results and discussion

Two main steps were followed to generate a detailed geological image map for Bulghah gold mine area. In the first step, the authors prepared and generated a 3/2, 4/2, and 4/3 SPOT band ratio images in addition to a false color composite ratio image using Geomatica PCI software. While during the second step, the lithological units with their image signatures and colors are verified, checked, and modified using field observations. The above FCC ratio image gives the best lithologic discrimination in which gossan, marble, Hulayfah volcanics, diorite–tonalite, gneissose granite, and alkali granite exhibit sky blue, blood red, bluish light brown, orange, brick red, and deep blue colors, respectively.

Structural information extracted from the visually examined panchromatic SPOT imagery, published geological maps, and field check were used to develop the detailed structural map for the study area. The following four main fault systems were recognized affecting the study area: (1) N–S strike-slip Nabitah belt, (2) NW–SE left lateral strike-slip Najd fault system, (3) E–W trending faults, and (4) NE–SW trending fault system. Dyke swarms with different directions and widths crosscut diorite–tonalite and other granitic intrusions in the study area. Barnicoat et al. (1998) try to establish the nature of any structural controls on gold mineralization in the Bulghah prospect. They studied the geological history of the prospect as well as the structures hosting the mineralization. They concluded that Bulghah central and the surrounding area have undergone several different deformational episodes. Initial east–west crustal extension (phase 1) was followed at a later time by east–west crustal compression (phase 2). The final deformation event was characterized by north–south crustal extension (phase 3). Mineralization in the Bulghah gold mine was the result of structurally focused hydrothermal fluid that occurred during regionally extensive crustal extensional deformation and associated cataclastic fault development (Barnicoat et al. 1998).

Conclusions

This study presents a new geological image map (scale 1:10,000) for Bulghah gold mine area that delineates new extensions for the diorite–tonalite intrusion generated using

the processed SPOT 5 data in collaboration with field observations. 3/2, 4/2, and 4/3 band ratio images discriminate successfully the different rock units which cover the study area. Diorite–tonalite intrusion has dark gray and gray image signatures on 4/3 and 4/2 band ratio images, respectively. IHS fusion technique is used to generate a large-scale informative imagery used for diorite–tonalite intrusion delineation. High spatial resolution SPOT panchromatic imagery is utilized for detailed structural mapping. From the field observations, it is revealed that the study area is affected by the older N–S Nabitah and the younger NW–SE Najd fault systems. Finally, this study reveals the usefulness of SPOT 5 data, to a great extent, for geological mapping and mineral exploration.

References

- Agar RA (1992) The Tectono-Metallogenic Evol of the Arab Shield: Precambrian Res 58:169–194
- Albino GV, Jalal S, Christensen K (1995) Neoproterozoic mesothermal gold mineralization at Sukhaybarat East mine, Saudi Arabia. Trans Inst Mining Metall, Sect B 104:157–170
- Al Jahdali NS (2004) Geology of Jabal Ghadara area, Bir Tawila District with special emphasis on listvenite as a potential source for gold in the Kingdom of Saudi Arabia. Unpublished M.Sc. Thesis, King Abdul Aziz University, Jeddah, Saudi Arabia
- Al Shanti AMS, Mitchell AHG (1976) Late Precambrian subduction and collision in the Al Amar-Idzas region, Arabian Shield, Kingdom of Saudi Arabia. Tectonophysics 30:T41–T47
- Bakor AR, Gass IG, Neary C (1976) Jabal Al Wask, Northwes Saudi Arabia, an Eocambrian back-arc ophiolite. Earth Planet Sci Lett 30:1–9
- Barnicoat AC, Freeman SR, Henderson IHC, Phillips GM (1998) Structural controls on gold mineralization in the Bulghah prospect. Rock Deformation Research – Leeds University, Report 03
- Camp VE (1984) Island-arcs and their role in the evolution of the Western Arabian Shield. Geol Soc Am Bull 95:913–921
- Carper WJ, Lillesand TM, Kiefer RW (1990) The use of intensity–hue–saturation transformation for merging SPOT panchromatic and multispectral image data. Photogramm Eng Remote Sens 56:549–467
- Chavez PS, Sides SC, Anderson JA (1991) Comparison of three different methods to merge multiresolution and multispectral data: Landsat TM and SPOT panchromatic. Photogramm Eng Remote Sens 57:295–303
- Delfour J (1977) Geology of the Nuqrah quadrangle, sheet 25E. Kingdom of Saudi Arabia, D.G.M.R., Geologic Map GM-28, scale 1:200 000, 32p
- Delfour J (1981) Geologic, tectonic and metallogenic evolution of the northern part of the Arabian Shield (Kingdom of Saudi Arabia). Bulletin du bureau de Recherches et Minières (deuxieme serie).; (1–2) Section II, pp. 1–19
- Drury S (1993) Image interpretation in geology. 2nd edition. Chapman and Hall, London
- Eberte JM, Sahl M (1999) Sukhaybarat gold deposit and mine. IUSGS/ UNESCO Deposit Modeling Workshop. Field trip guide book. Jeddah, Kingdom of Saudi Arabia. 24 pp
- Ehlers M (1991) Multisensor image fusion techniques in remote sensing. Photogrammetry and remote sensing 46:19–30
- Frisch W, Al Shanti A (1977) Ophiolite belts and the collision of island arcs in the Arabian Shield. Tectonophysics 43:293–306

- Gass IG (1977) The evolution of the pan-African crystalline basement in NE Africa and Arabia. *J Geol Soc Lond* 134:129–138
- Gass IG (1981) Pan-African (Upper Proterozoic) plate tectonics of the Arabian-Nubian Shield. In: Kröner A (ed) *Precambrian Plate Tectonics*. Elsevier, Amsterdam, pp 387–405
- Garguet-Duport B, Girel J, Chaassery J, Pautou G (1996) The use of multiresolution analysis and wavelets transform for merging SPOT panchromatic and multispectral image data. *Photogramm Eng Remote Sens* 62:1057–1066
- Greenwood WR, Hadley DG, Anderson RF, Fleck RJ, Schmidt DL (1976) Late Proterozoic cratonization in southwestern Saudi Arabia. *Royal Soc of Lond Philos Trans Ser A* 280:517–527
- Harbi HM (2004) Genesis of gold mineralization at Zalm area, Central Saudi Arabia; K.S.A. 6th Intern. Conf. on Geochemistry, Alex. Univ. Egypt, P. 143–160
- Harbi HM, McNaughton N (2011) Geochronological investigation of gold-hosted intrusive rocks within the Afif Terrane, Arabian Shield; Saudi Arabia. (In preparation)
- Leistel JM, Al Jahdali N, Khalil I, Kattu G, Eberle JM, Lambert A, Siddiqui A, Saleh Y (1999) Results of precious metal exploration in the Zalm prospect, Kingdom of Saudi Arabia: Saudi Arabian Deputy Ministry for Mineral Resources Technical Report BRGM-TR-99-14, 39 p. 108.
- Li S, Kwork JT, Wang Y (2002) Using the discrete wavelet frame transform to merge Landsat TM and SPOT panchromatic images. *Information Fusion* 3:17–23
- Pohl C, Van Genderen JL (1998) Multisensor image fusion in remote sensing: concepts, methods, and applications. *Int J Remote Sens* 19:823–854
- Sabir H (1989) The metallogeny of gold deposits in Saudi Arabia and its significance in gold exploration and exploitation, *Jour. King Abdulaziz Univ, Earth Sci* 3:145–156
- Schmidt DL, Hadley DG, and Stoesser DB (1979) Late Proterozoic history of the Arabian Shield South Najd Province, Kingdom of Saudi Arabia, In S.A. Tahoun (ed.), *Evolution and mineralization of the Arabian Shield*, King Abdulaziz University, Jeddah, *Institute of Applied Geology Bulletin*, 2: p.44–58
- Wald L (2002) *Data fusion definitions and architectures: fusion of images of different spatial resolutions*. Les presses de l'Ecole des mines, Paris